

MARS and G4beamline simulations: momentum and spin tracking from the production target to the extraction point from the Delivery Ring

V. Tishchenko* and W.M. Morse

Brookhaven National Laboratory, Upton, NY 11973, USA

J.-F. Ostiguy and J. Morgan

Fermi National Accelerator Laboratory, Batavia, IL 60510, USA

M.J. Syphers

Michigan State University, East Lansing, MI 48824, USA

(muon ($g-2$) collaboration)

(Dated: February 26, 2014)

Abstract

MARS and G4beamline programs were used to simulate pion production in the ($g-2$) production target, pion collection by the Lithium lens, pion decay, muon collection by the beamline optics and momentum and spin tracking up to the extraction point from the Delivery Ring. The calculated number of magic-momentum muons ($\Delta p/p = \pm 0.5\%$) per proton on target after five turns around the Delivery Ring is about 1.7×10^{-7} , the polarization of the beam of magic-momentum muons is about 95%.

* vtishchenko@bnl.gov; <https://pubweb.bnl.gov/~vtishchenko>

I. INTRODUCTION

This work continues our previous studies of beam transport through the E989 beamline [1]. The former `G4beamline` model of the E989 beamline was improved by making the field of the injection kicker time dependent which made it possible to track the beam around the Delivery Ring (DR) for multiple turns without the need to restart simulations after the first turn. In this work we use `MARS` [2] to simulate pion production in the target and focusing by the Li-lens.

II. MARS MODEL

A cartoon of the E989 target station is shown in Fig. 1 as implemented in the `MARS` model in [3] and used in this work. The primary proton beam with kinetic energy of 8 GeV impinges on the pion production target (1), which is a vertical 12.7-cm-diameter cylinder with a chord along the proton beam axis of about 7.5 cm in the inconel layer. A secondary beam of charged particles produced in the target is focused by the 16-cm-long 2-cm-diameter Li-lens with 230 T/m magnetic field gradient. Charged particles (π^+ , μ^+ , K^+) entering a virtual detector (3) installed at the downstream face of the Li-lens are dumped into a file on disk for further tracking in `G4beamline`.

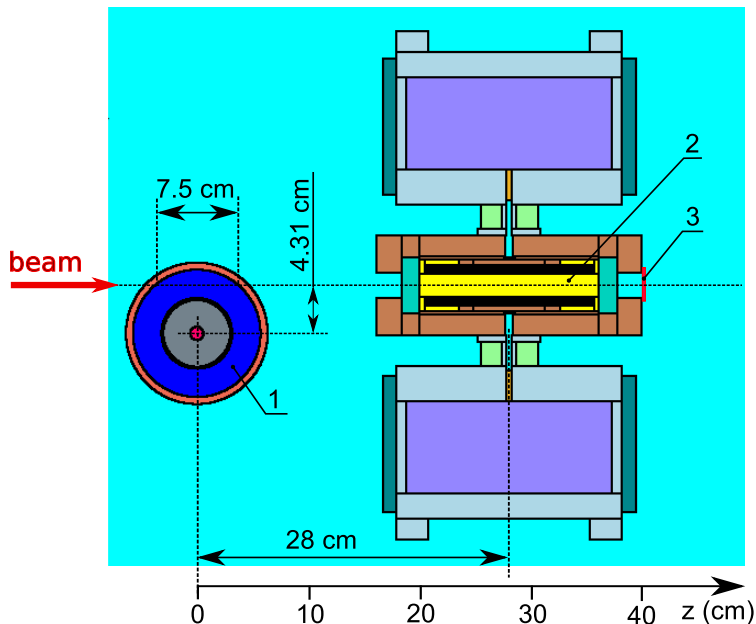


FIG. 1: `MARS` model of the E989 target station (top view): inconel target (1), 16-cm-long 2-cm-diameter Li cylinder with magnetic field (2), virtual detector, $z = 40$ cm (3).

The primary proton beam starts 5 cm upstream from the target and has Gaussian spatial and angular distribution. The parameters of the distributions are adjusted such that in the absence of the target the beam is focused at $z = 0$ to form a spot with $\sigma_x = \sigma_y = 0.55$ -mm and $\sigma_{x'} = \sigma_{y'} = 0.38$ -mrad. As discussed elsewhere, a proton beam with smaller radius, a Li-lens with stronger focusing field and placed closer to the production target will improve the efficiency of pion capture. However, in this note we use the “default” parameters without making any optimizations Li-lens position or current.

III. G4BEAMLIN MODEL

To track the beam from the downstream face of the Li-lens to the upstream end of the $(g - 2)$ inflector we use `G4beamline` simulation program [4]. The `G4beamline` model of the E989 beamline is described in our previous note [1]. For the studies in this note we extended the model in [1] by implementing a time-dependent field in the injection kicker which switches off after the first turn of the beam around DR to allow the beam to travel multiple times around the DR. In this note we tracked the beam up to five turns around the DR. As before, the last section (M4) has not been implemented yet in the model, therefore we do not discuss beam extraction and final tracking to the $(g - 2)$ ring. However, we do not expect the beam properties to change appreciably by passing through the final section of the beamline.

Another change in the model is related to the magnet geometry. We found that the `Septum` magnet was too thick vertically, so the beam hit it on the second turn (see Fig. 2). For the studies in this note we reduced the vertical thickness of the `Septum` magnet from 200 mm to 51 mm to create sufficient clearance between the magnet steel and the circulating beam in the DR (bottom picture in Fig. 2). However, the model of the `Septum` magnet may not be correct and requires additional verification.

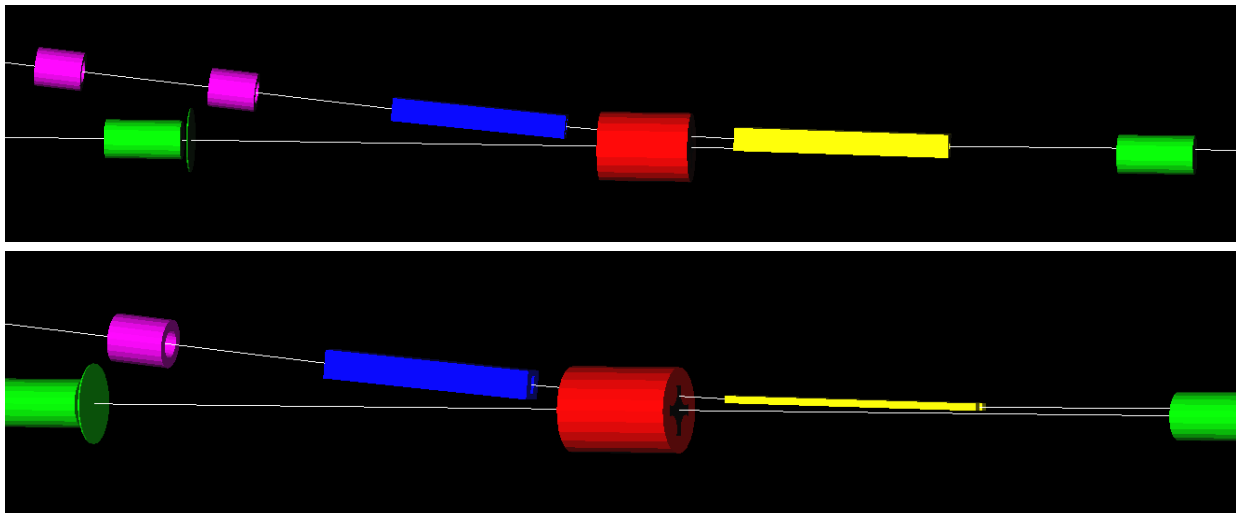


FIG. 2: `G4beamline` model of the injection lattice into the Delivery Ring: C-Magnet (blue), Q303 (Red), Septum (yellow), virtual `STOP` detector (thin green disc). The thick Septum magnet in the original version of the model did not allow the beam to make more than one turn around the Delivery Ring (top picture). Reducing the vertical size of the magnet from 200 mm to 51 mm resolved the problem (bottom picture).

To record the beam particles for the offline analysis we installed two virtual detectors, a `START` detector at $z = 5$ mm downstream from the Li-lens and a `STOP` detector at the end of a complete turn around the DR (thin green disc in Fig. 2).

As was mentioned in [1], the arms of the Star chambers in our model were longer than they should be because of limitations in `G4beamline` (See Fig. 3 in [1]). To slightly improve our model we added cylindrical beampipes with inner radius of 74 mm between the magnets. However, this may not be sufficient and our model will overestimate the admittance.

Finally, as we have already mentioned, for the studies in this note we use `MARS`-generated

particles as input for the `G4beamline` simulations.

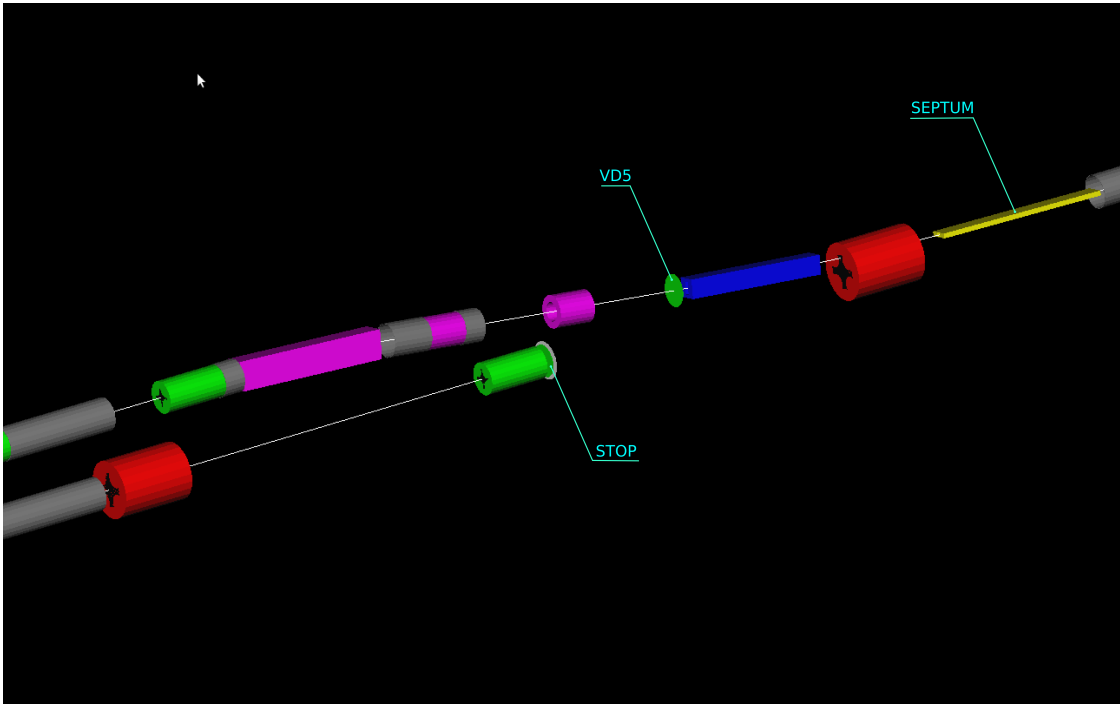


FIG. 3: Location of virtual detectors near the injection point into the Delivery Ring. `G4beamline` model of the E989 beamline.

IV. SIMULATIONS

Using the Fermigrid computer facility at Fermilab we simulated 1.47×10^{10} protons on target (POT) in `MARS`. These produced approximately 1.1×10^7 hits in the virtual START detector by particles with momentum in the range (2.7 ÷ 3.5 GeV) (mostly π^+ , some K^+ and μ^+ ; other species we ignored). The horizontal (x) and vertical (y) phase space distributions of particles in the START detector are shown in Fig. 4. We use a very relaxed phase space cut to select `MARS` data for tracking in `G4beamline`, ± 20 mm in x and y and ± 20 mrad in x' and y' .

V. BEAM TRANSMISSION

To study the beam transmission through the beamline elements we disabled the decay of unstable particles in `G4beamline`. Therefore, beam particles can be lost only if they hit a beamline element.

The phase space distribution of transmitted pions in the START detector are shown in Fig. 5. The emittance of the transmitted pion beam is about 40π mm·mrad which is in agreement with the beamline design.

The momentum distribution of pions in the three virtual detectors is shown in Fig. 6. We remind the reader about the relaxed phase space cut in `MARS` which leads to a large number of hits in the START detector. Since we are interested in the absolute number of

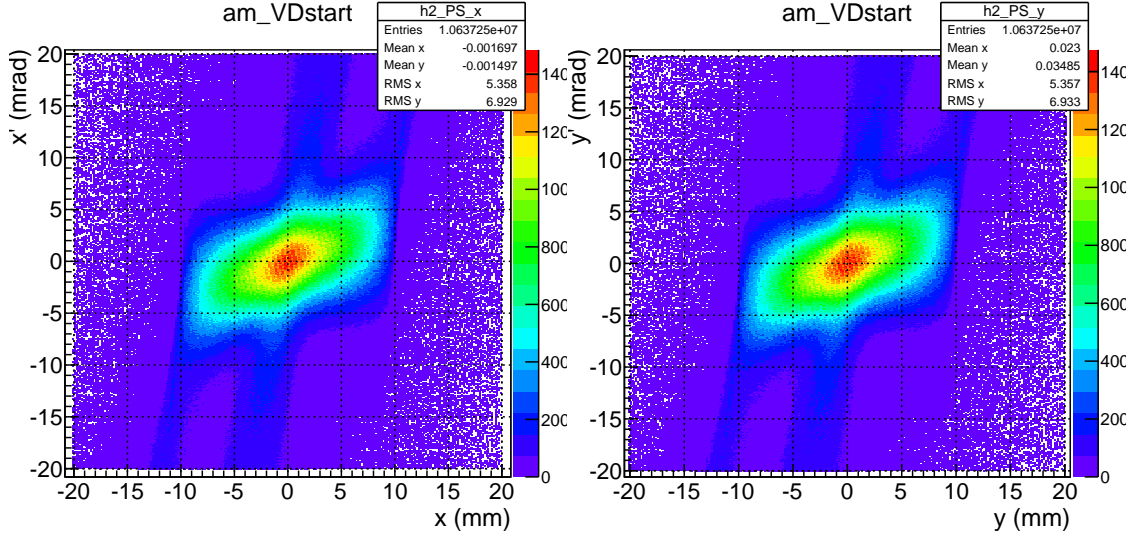


FIG. 4: Horizontal (left) or vertical (right) phase space distributions of particles in the START detector.

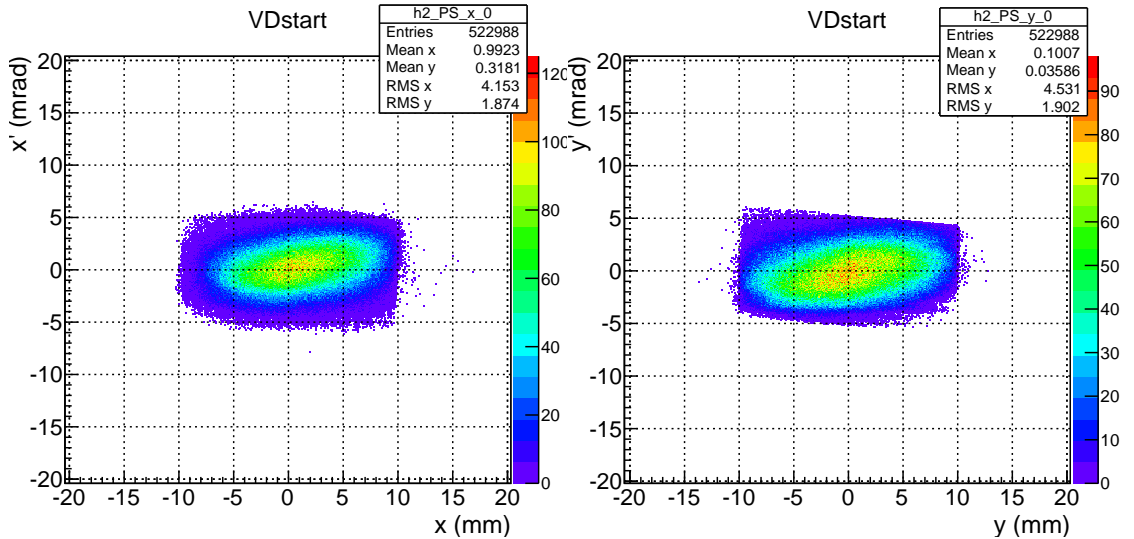


FIG. 5: Horizontal (left) or vertical (right) phase space distributions of transmitted pions in the START detector. Pion decay disabled.

particles downstream in the beamline, we did not apply any additional artificial cuts to limit the emittance of the beam. Particle transmission is defined by the beamline lattice and the natural apertures of the beamline elements without misalignment. The number of pions per POT in the momentum band $\Delta p/p = \pm 5\%$ in VD5 is 9.3×10^{-5} . This number is in a reasonable agreement with former estimates based on MARS-simulated data¹.

¹ In Fig. 7.10 in CDR [5] the pion yield for $|\Delta p/p| = 2\%$, $\sigma_x = \sigma_y = 0.55$ mm and achievable β is approximately 3.2×10^{-5} . Therefore the number of pions scaled to the $|\Delta p/p| = 5\%$ band is 8×10^{-5} . Small discrepancy can be attributed to slightly higher than 40π mm-mrad admittance of the beamline discussed above.

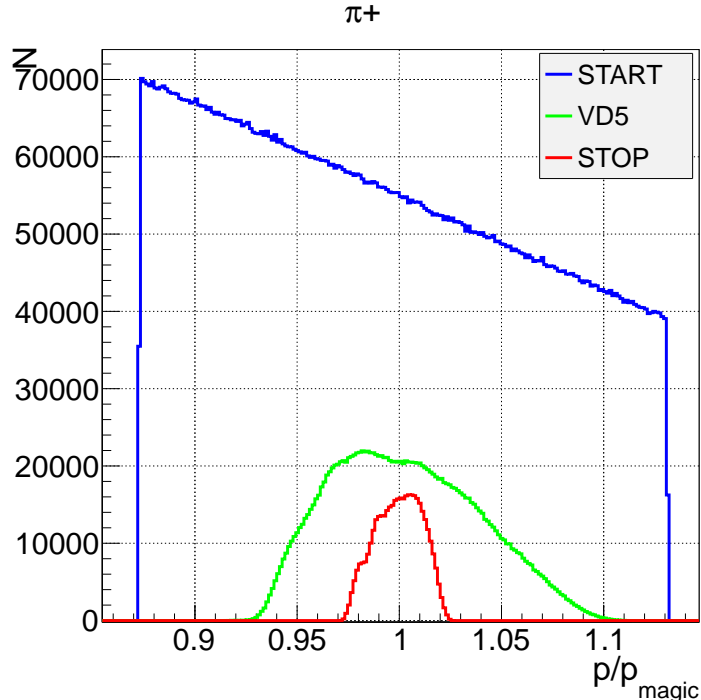


FIG. 6: Momentum distribution of pions in START (blue), STOP (red) and VD5 virtual detectors (green). Pion decay disabled.

VI. MUON COLLECTION

For the studies in this and the following sections we enable stochastic processes in `G4beamline` including particle decay. The momentum distributions of muons in the three virtual detectors is shown in Fig. 7. The number of magic-momentum muons ($\Delta p/p = \pm 0.5\%$) in the STOP detector is plotted in Fig. 8 as function of the number of turns around DR (red symbols). Also shown the total number of survived pions (blue symbols). After one turn, the pion contamination of the muon beam is relatively high, therefore more than one turn will be needed to clean the beam from pions. Due to decay, the number of usable muons decreases with the number of turns. The optimum number of turns should be found as a compromise between the absolute number of usable muons, pion to muon ratio and proton-muon separation in time. Protons will not be discussed in this note.

If we take five turns of the beam around DR and lossless beam extraction from the DR and full transmission through the final beamline section, the estimated number of magic-momentum muons ($\Delta p/p = \pm 0.5\%$) at the upstream face of the $(g - 2)$ inflector will be roughly 1.5×10^{-7} per proton on target or 1.5×10^5 muons per fill.

VII. BEAM POLARIZATION

The distribution of horizontal components of the polarization of magic-momentum muons ($\Delta p/p = \pm 0.5\%$) in the STOP detector is shown in Fig. 9. The average polarization is approximately 95%. This includes approximately 5% of upstream-born muons (i.e. muons originated in the pion production target, Li-lens and in the space between the target and

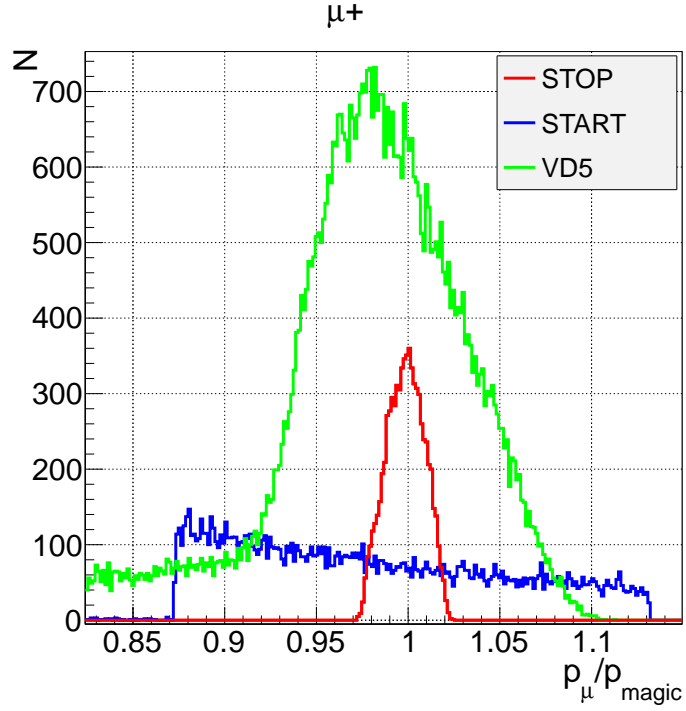


FIG. 7: Momentum distribution of muons in START (blue), STOP (red, five turns around DR) and VD5 virtual detectors (green).

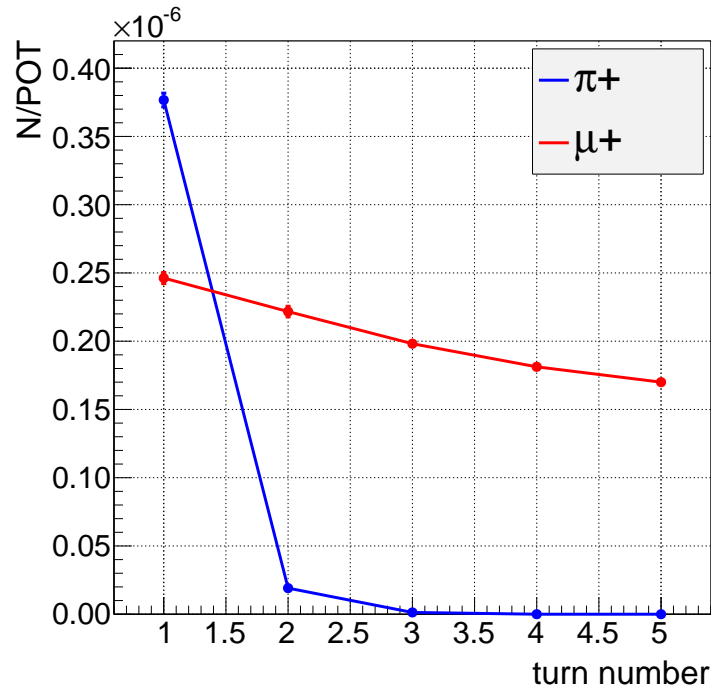


FIG. 8: Number of particles in the STOP detector as function of the number of turns around the DR, magic-momentum muons ($\Delta p/p = \pm 0.5\%$ around magic momentum, red symbols), or pions (blue symbols).

the Li-lens, see Fig. 1) which have low ($\approx 55\%$) polarization. The horizontal components of the polarization of upstream magic-momentum muons are shown in the bottom row in Fig. 9.

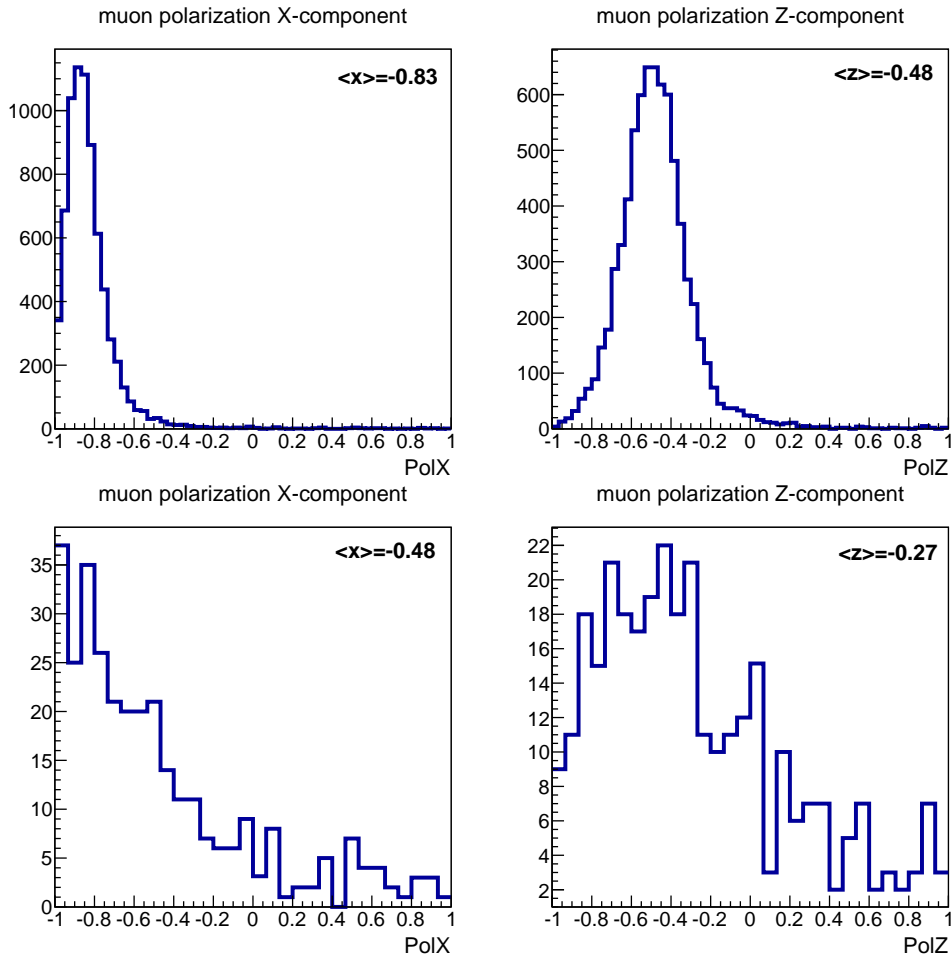


FIG. 9: Horizontal components of the polarization of magic-momentum muons ($\Delta p/p = \pm 0.5\%$) in the STOP detector; all muons (top) or muons originated in the Li-lens and upstream (bottom).

The upstream muons consist of both, direct muons due to proton-nucleus interactions and secondary muons from π^+ , K^+ , etc. weak decays. Their momentum distribution is shown in Fig. 10.

Since the standard **MARS** code does not calculate or track particle spin, we had to implement this feature ourselves to obtain the polarization of upstream muons. However, since **MARS** is a closed source, there is no confidence that everything was done correctly, in particular, in the case of weak decay of kaons.

VIII. SUMMARY

This work continues our previous simulations of the beam transport through the E989 beamline [1]. A brief summary of new features of the beamline model includes:

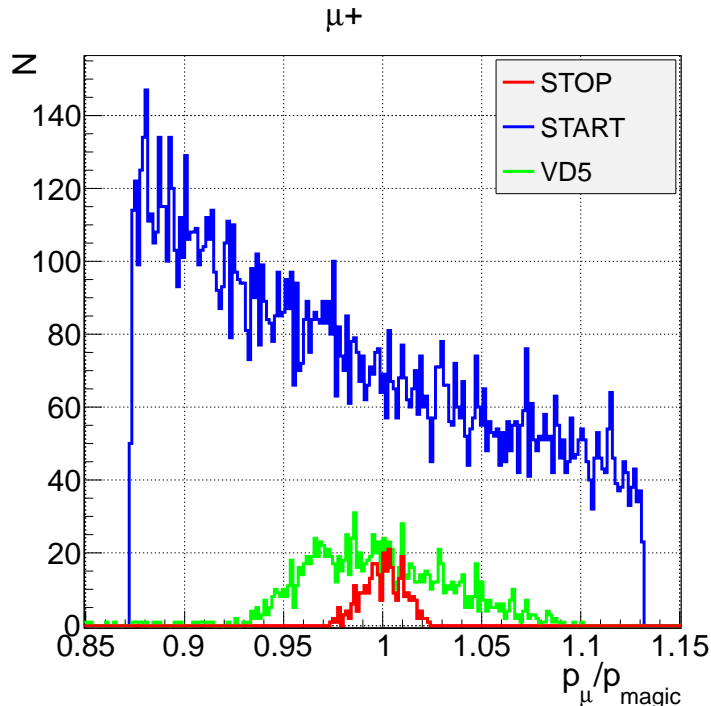


FIG. 10: Momentum distribution of muons in the STOP detector originated in and upstream of the Li-lens.

- Time-dependent injection kicker which allows beam tracking around the Delivery Ring for multiple turns.
- Beampipes to partially correct for the deficiency in the model of star vacuum chambers.
- MARS-generated particles from pion-nucleus interaction in the target (and Li-lens).
- Polarization of upstream muons.

We also observed a problem in the model of the Septum magnet not allowing the beam to circulate more than one turn in the Delivery Ring. The quick fix was to reduce the height of the magnet, but we will continue to investigate this problem.

Using Fermigrid we simulated 1.47×10^{10} events of proton-target interactions in MARS. MARS-generated secondary beam was tracked for up to five turns around the Delivery Ring using G4beamline. The calculated number of magic-momentum muons ($\Delta p/p = \pm 0.5\%$) after five turns around the Delivery Ring is 1.7×10^5 per fill; the polarization of the magic-momentum muon beam is approximately 95%.

-
- [1] V. Tishchenko, W. M. Morse, J. F. Ostiguy, and J. Morgan, *Simulation of Beam Transport Through M2-M3-DR Beamline in G4beamline: first results*, E989 note 1228 (Fermi National Accelerator Laboratory, 2013).
- [2] N.V. Mokhov, "The Mars Code System User's Guide", Fermilab-FN-628 (1995); O.E. Krivosheev, N.V. Mokhov, "MARS Code Status", Proc. Monte Carlo2000 Conf., p. 943, Lisbon,

- October 23-26, 2000; Fermilab-Conf-00/181 (2000); N.V. Mokhov, "Status of MARS Code", Fermilab-Conf-03/053 (2003); N.V. Mokhov, K.K. Gudima, C.C. James et al, "Recent Enhancements to the MARS15 Code", Fermilab-Conf-04/053 (2004); <http://www-ap.fnal.gov/MARS/>.
- [3] C. Yoshikawa, C. Ankenbrandt, A. Leveling, N. Mokhov, J. Morgan, D. Neuffer, and S. Striganov, in *Proceedings of IPAC2012, New Orleans, Louisiana, USA* (2012) iISBN: 78-3-95450-115-1.
- [4] T. Roberts and D. Kaplan, in *Particle Accelerator Conference, 2007. PAC. IEEE* (2007) pp. 3468 –3470.
- [5] E989 Collaboration, *Muon ($g - 2$) Conceptual Design Report*, Tech. Rep. (Fermi National Accelerator Laboratory, 2013).